The Plant Cell, Vol. 26: 3693–3708, September 2014, www.plantcell.org

How Vacuolar Sorting Receptor Proteins Interact with Their Cargo Proteins: Crystal Structures of Apo and Cargo-Bound Forms of the Protease-Associated Domain from an *Arabidopsis* Vacuolar Sorting Receptor[W]

Fang Luo,[a,b] Yu Hang Fong,[a] Yonglun Zeng,[b] Jinbo Shen,[b] Liwen Jiang,[b] and Kam-Bo Wong[a,b,1]

[a] Centre for Protein Science and Crystallography, The Chinese University of Hong Kong, Shatin, New Territories, Hong Kong, China
[b] Centre for Cell and Developmental Biology and State Key Laboratory of Agrobiotechnology, School of Life Sciences, The Chinese University of Hong Kong, Shatin, New Territories, Hong Kong, China

In plant cells, soluble proteins are directed to vacuoles because they contain vacuolar sorting determinants (VSDs) that are recognized by vacuolar sorting receptors (VSR). To understand how a VSR recognizes its cargo, we present the crystal structures of the protease-associated domain of VSR isoform 1 from *Arabidopsis thaliana* (VSR1PA) alone and complexed with a cognate peptide containing the barley (*Hordeum vulgare*) aleurain VSD sequence of $_{1}$ADSNPIRPVT$_{10}$. The crystal structures show that VSR1PA binds the sequence, Ala-Asp-Ser, preceding the NPIR motif. A conserved cargo binding loop, with a consensus sequence of $_{95}$RGxCxF$_{100}$, forms a cradle that accommodates the cargo-peptide. In particular, Arg-95 forms a hydrogen bond to the Ser-3 position of the VSD, and the essential role of Arg-95 and Ser-3 in receptor-cargo interaction was supported by a mutagenesis study. Cargo binding induces conformational changes that are propagated from the cargo binding loop to the C terminus via conserved residues in switch I-IV regions. The resulting 180° swivel motion of the C-terminal tail is stabilized by a hydrogen bond between Glu-24 and His-181. A mutagenesis study showed that these two residues are essential for cargo interaction and trafficking. Based on our structural and functional studies, we present a model of how VSRs recognize their cargos.

INTRODUCTION

The secretory pathway in animal, yeast, and plant cells shares common endomembrane compartments, including endoplasmic reticulum, Golgi apparatus, trans-Golgi network (TGN), prevacuolar compartment (PVC)/endosome, and the vacuole/lysosome within the endomembrane system (Neuhaus and Rogers, 1998; Jørgensen et al., 1999; Ghosh et al., 2003; De Marcos Lousa et al., 2012). Within the lumen of the endomembrane system, delivery of soluble proteins to the lysosome/vacuole of these three types of cells shares a common theme: An integral membrane receptor protein recognizes cargos and delivers them to a PVC/endosome, where the cargo protein dissociates from the receptor (Kirsch et al., 1994; Cereghino et al., 1995; Cooper and Stevens, 1996; Paris et al., 1997; Robinson and Hinz, 1997; Jiang and Rogers, 1998; Wang et al., 2011). Unlike animal cells, which recognize a post-translational modification, mannose-6-phosphate, as the lysosomal sorting signal, plant, and yeast cells use sequence-specific information known as vacuolar sorting determinants (VSDs) as their vacuolar sorting signal (Nakamura and Matsuoka, 1993; Cereghino et al., 1995; Paris et al., 1997; Jiang and Rogers, 1998; Neuhaus and Rogers, 1998; Ahmed et al., 2000; Motyka et al., 2000; Humair et al., 2001; Olson et al., 2002; Ghosh et al., 2003; daSilva et al., 2005, 2006; Vitale and Hinz, 2005; Suen et al., 2010).

Vacuolar sorting receptor (VSR) proteins are responsible for recognizing the VSDs on the cargo-proteins and targeting them to the vacuole (Nakamura and Matsuoka, 1993; Paris et al., 1997; Jiang and Rogers, 1998; Neuhaus and Rogers, 1998; Vitale and Raikhel, 1999; Ahmed et al., 2000; Vitale and Hinz, 2005). BP-80 from pea (*Pisum sativum*) was the first VSR protein identified, which binds to a NPIR-containing sequence motif located at the N-terminal region of aleurain (Kirsch et al., 1994; Paris and Neuhaus, 2002; Paris et al., 1997; Humair et al., 2001). The NPIR-containing sequence motif is the most well studied VSD and is found in a number of vacuolar targeting proteins (Matsuoka and Nakamura, 1991, 1999; Holwerda et al., 1992; Kirsch et al., 1994, 1996; Paris et al., 1997; Ahmed et al., 2000; Humair et al., 2001; Watanabe et al., 2002, 2004; Shimada et al., 2003; Suen et al., 2010; Shen et al., 2013). Mutagenesis studies have revealed that receptor-cargo recognition is sequence specific (Matsuoka et al., 1995; Kirsch et al., 1996; Shimada et al., 1997; Matsuoka and Nakamura, 1999; Suen et al., 2010). For example, I-to-G substitution of the NPIR motif in sporamin and aleurain affects vacuolar sorting and receptor binding (Kirsch et al., 1996; Matsuoka and Nakamura, 1999; Ahmed et al., 2000). In addition to the N-terminal NPIR-containing motif, it has been reported that VSRs also recognize sequence motifs located at the C terminus (Kirsch et al., 1996; Shimada et al., 1997; Jolliffe et al., 2004; Suen et al., 2010).

VSRs are type I integral membrane proteins that contain an N-terminal lumenal region (NT), a single transmembrane domain (TMD), and a C-terminal cytoplasmic tail (CT) (Kirsch et al., 1994;

[1] Address correspondence to kbwong@cuhk.edu.hk.
The author responsible for distribution of materials integral to the findings presented in this article in accordance with the policy described in the Instructions for Authors (www.plantcell.org) is: Kam-Bo Wong (kbwong@cuhk.edu.hk).
[W] Online version contains Web-only data.
www.plantcell.org/cgi/doi/10.1105/tpc.114.129940

Paris et al., 1997; Neuhaus and Rogers, 1998) (Supplemental Figure 1). The TMD and CT domains are responsible for targeting the VSR to the vacuole in plant cells (Tse et al., 2004; daSilva et al., 2006; Miao et al., 2006; Foresti et al., 2010). When fused to the TMD and CT domains of *Arabidopsis thaliana* VSR1-7, the green fluorescent protein (GFP) constructs localized to PVC in untreated cells or in vacuolated PVCs in wortmannin-treated cells (Miao et al., 2006). The TMD and CT domains are also responsible for homomeric interaction of *Arabidopsis* VSR1, which is essential to its trafficking to the PVC (Kim et al., 2010). The CT domain of all VSRs contain a consensus sequence motif, YMPL, that is recognized by the AP-1 clathrin adaptor protein complex and is involved in the formation of clathrin coated vesicles. According to a frequently cited model, the cargo-VSR complex is sequestered into clathrin coated vesicles at the TGN and delivered to the PVC. Recycling of VSRs back to Golgi/TGN is mediated by the retromer complex (daSilva et al., 2005, 2006; Lam et al., 2006; Foresti et al., 2010). However, evidence is accumulating showing that VSR-cargo interactions occur much earlier in the endomembrane system and that retromer may recycle VSRs from a maturing TGN (Robinson, 2014).

The lumenal region of VSRs is responsible for specific cargo-receptor interactions at the Golgi/TGN (Cao et al., 2000; Watanabe et al., 2004). This region contains three domains: a protease-associated (PA) domain at the N terminus, a Central domain in the middle, and three epidermal growth factor repeats (EGF) at the C terminus (Supplemental Figure 1). The PA domain is homologous to the lumenal region of receptor-homology-transmembrane-RING-H2 (RMR) protein, which is also involved in protein sorting in plant cells (Cao et al., 2000; Shen et al., 2011; Wang et al., 2011). For example, the RMR isoform 1 of *Arabidopsis* (RMR1) is involved in the transport of phaseolin to a PSV-like compartment, suggesting that the PA domain is involved in cargo-receptor interactions (Park et al., 2005). Both the PA and the Central domains are involved in cargo-receptor interaction in VSRs. A protease-digested fragment containing the PA and Central domains of BP-80 from pea can recognize the NPIR motif of aleurain. On the other hand, a fragment containing the Central domain and the EGF repeat binds the aleurain in a non-NPIR-specific manner (Cao et al., 2000). The role of the EGF repeats is not fully understood, but it is believed that they may serve as a calcium binding domain and modulate the ligand binding of VSRs by inducing the conformational changes in the PA and the Central domain (Cao et al., 2000; Watanabe et al., 2002, 2004).

The underlying molecular mechanism of how VSR proteins bind to their cargo proteins remains elusive. It has been reported previously that crystals could be obtained for the lumenal region of BP-80, but the structure of VSR remains unknown (Rogers et al., 2004). Here, we report the crystal structures of the PA domain of *Arabidopsis* VSR1 (VSR1PA) in apo form and in a complex with its cognate aleurain cargo-peptide. We show that the VSR1PA is responsible for recognition of a sequence preceding the NPIR motif and that cargo binding induces large conformational changes in VSR1PA. Supported by mutagenesis and functional studies, we propose a model of how VSRs recognize their cargo proteins.

RESULTS

Crystal Structures of VSR1PA in the Apo- and Cargo-Peptide Binding Forms

To understand how VSRs recognize their cargo proteins, we determined the crystal structures of the PA domain of *Arabidopsis* VSR1 (VSR1PA) in the apo form and in complex with its cognate peptide ($_{1}$ADSNPIRPVT$_{10}$) from the cargo-protein aleurain (Figure 1, Table 1). The PA domain of the VSR protein is built from a seven-stranded barrel surrounded by six peripheral helices, which is a typical fold common to PA domains from various species (Brown et al., 2005; Ottmann et al., 2009). Sequence alignment showed that the PA domain is highly conserved among various VSRs (Supplemental Figure 2A). Notably, the conserved residues are mainly located on one side of the PA domain and clustered around the cargo binding site (Supplemental Figure 2B).

The structure of VSR1PA in complex with its cognate peptide reveals that VSR1PA binds the first three residues ($_{1}$Ala-Asp-Ser$_{3}$) of the aleurain cargo-peptide (Figure 1B). The peptide residues $_{4}$NPIRPVT$_{10}$ do not have an interpretable electron density and are presumed to be disordered (Supplemental Figure 3). As indicated by the large values of Cα displacement, large conformational changes are found in four regions: the switch I (residue 20-27), the switch II (residue 44-53), the switch III (residue 126-144), and the switch IV regions (residue 174-182) (Figure 1C). Residues 20-22 (switch I) and 132-138 (switch III) became disordered upon binding of cargo-peptide (Figure 1B).

VSR1PA Interacts with the Backbone Amide of the Cargo-Peptide

Two loops of VSR1PA, namely, the cargo binding loop ($_{95}$RGDCYF$_{100}$) and the switch III loop, form a binding cavity to accept the peptide ligand (Figure 1D). The cargo binding loop is located between β4 and α3, while the switch III loop is formed by uncoiling of α4 ($_{125}$LITM$_{128}$) upon cargo binding (Figures 1A and 1B). Both the cargo binding and the switch III loops form hydrogen bonds to the backbone amide groups of the peptide ligand: Ala-1 of the peptide ligand forms interaction with Thr-127 and Asp-129, Asp-2 with Phe-100, and Ser-3 with the side chain of Arg-95 (Figure 1D).

Binding of Cargo Induces a Swivel Motion at the C Terminus of VSR1PA

The cargo binding loop and switch I, II, III, and IV are interconnected by a hydrogen bond network (Figures 2A and 2B). In the apo form of VSR1PA, residues R20-V22 of switch I form hydrogen bonds with I44/N46 of switch II and D129/D124 of switch III (Figure 2A). These hydrogen bonds hold the switch III residues in a position such that Glu-133 occupies the cargo binding site and forms hydrogen bonds to Arg-95 of the cargo binding loop (Figure 2A). Upon binding of the cargo-peptide, switch III residues (Glu-133 and Asp-134) are pushed away from the cargo binding site, thereby breaking the hydrogen bonds between switch I and III. As a result, residues R20-V22 (switch I) become unstructured and switch II moves toward switch III, allowing the formation of

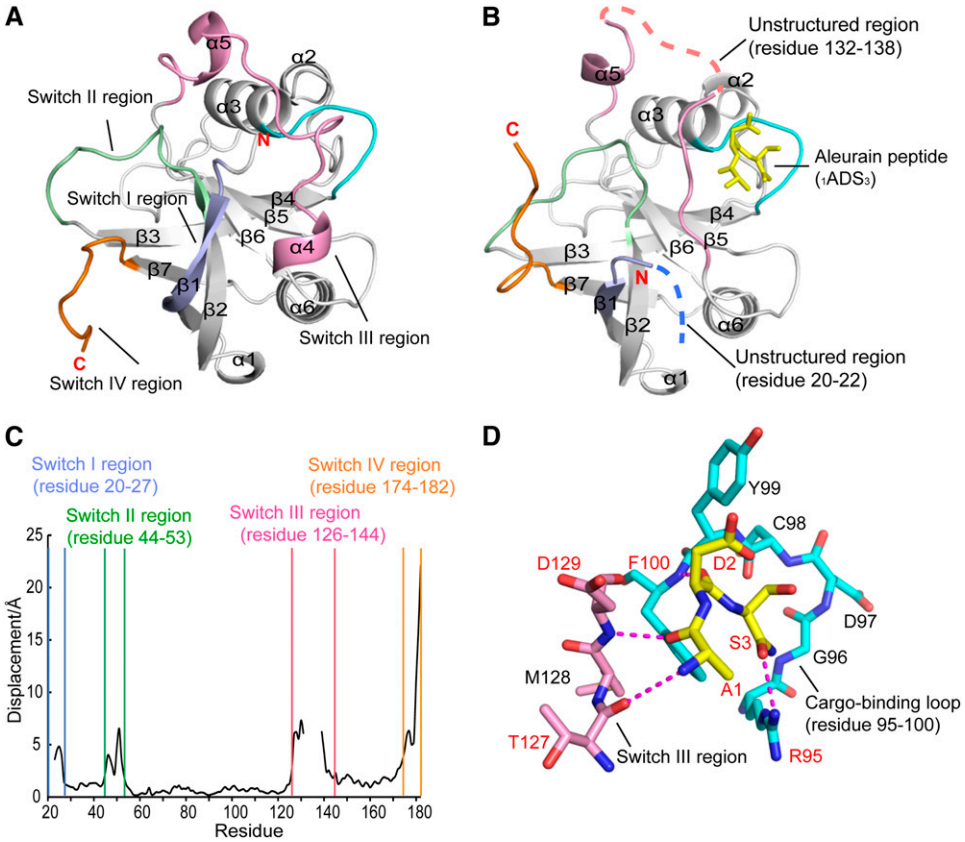

Figure 1. Crystal Structures of VSR1PA in the Apo Form and in Complex with Cognate Cargo-Peptide.

(A) and **(B)** Ribbon diagram illustrating the structures of VSR1PA in apo form **(A)** and in complex form **(B)**, with secondary structural elements labeled.
(C) Significant structural differences, as indicated by large values of Cα displacement, are found in four regions: switch I, II, III, and IV, which are color-coded blue, green, pink, and orange, respectively. In particular, residues 20-22 (switch I) and residues 132-138 (switch III) become unstructured upon binding of cargo peptide.
(D) Receptor-cargo interaction in VSR1PA. The cargo binding loop (R95-F100; cyan) and the switch III residues (T127-D129; pink) form a binding cavity that accepts the cargo peptide (yellow). The backbone amides of the cargo peptide form hydrogen bonds (dashed lines) to the side chain of Arg-95, backbone amides of Phe-100, Thr-127, and Asp-129. Residues that participate in direct interaction are labeled in red, while others are labeled in black.

hydrogen bonds between Asn-46 (switch II) and Met-128/Asp-129 (switch III) in the complex structure (Figure 2B).

The cargo-induced conformational changes are propagated to switch IV via the interconnecting hydrogen bond network among switch I-IV (Figures 2A and 2B; Supplemental Movie 1 and Supplemental Figure 2C). In the apo form, the C terminus of VSR1PA is anchored to the switch I by a hydrogen bond between His-181 (switch IV) and Asn-26 (switch I) (Figure 2A). Due to the conformational changes in switch I upon cargo binding (see above), this hydrogen bond is broken and the switch IV undergoes a swivel motion that leads to an ~180° flip of the C terminus (Figure 2C). The flipped conformation is stabilized by a hydrogen bond between His-181 (switch IV) and Glu-24 (switch I) (Figure 2B).

Sequences Preceding the NPIR Motif Are Important in Receptor-Cargo Recognition and Trafficking

Our structural studies reveal that the PA domain of VSR1 plays a role in cargo recognition by forming backbone hydrogen bonds with the $_{1}$Ala-Asp-Ser$_{3}$ residues of the aleurain cargo-peptide (Figure 1D), suggesting the residues preceding the NPIR motif might play a role in receptor-cargo recognition. To test this hypothesis, we substituted each of these residues in the aleurain cargo-peptide with glycine (A1G, D2G, and S3G) and tested if these mutated peptides can interact with VSR1 (Figure 3). In vitro pull-down assay demonstrated that the N-terminal lumenal region of VSR1 (VSR1NT) could interact with the wild-type, A1G, and D2G aleurain peptides (Figure 3C). On the contrary, the S3G peptide failed to interact with VSR1NT (Figure 3C). We also included the I6G peptide as a control. It was previously shown that an I→G substitution in the NPIR motif abolishes binding with VSR (Kirsch et al., 1996; Matsuoka and Nakamura, 1999; Ahmed et al., 2000). Consistent with previous observations, the I6G peptide failed to pull down VSR1NT (Figure 3C). Similarly, VSR1NT was coimmunoprecipitated with wild-type aleu-VSD-GFP, but not with S3G-aleu-VSD-GFP and I6G-aleu-VSD-GFP (Figure 3D). Taken together, our results show that the S3G substitution abolished cargo-receptor binding.

Table 1. Diffraction Data Collection and Refinement Statistics

Crystal	Apo-VSR1PA	VSR1PA-Aleurain Peptide Complex
PDB code	4TJV	4TJX
Data collection		
Space group	$P12_11$	$P12_11$
Cell dimensions		
a,*b*,*c* (Å)	32.60, 62.68, 35.81	32.51, 58.65, 36.58
α, β, γ (°)	90.00, 109.39, 90.00	90.00, 90.65, 90.00
Wavelength (Å)	1.54187	1.54187
Resolution range (Å)	33.78-1.65 (1.69-1.65)	36.58-1.90 (1.95-1.90)
No. of unique reflections	15984 (1129)	10219 (616)
I/σI	74.0 (19.1)	21.5 (7.6)
Completeness	97.7 (94.9)	94.1 (85.4)
Redundancy	15.5 (15.2)	3.7 (3.6)
Rmerge	0.026 (0.148)	0.035 (0.134)
Refinement		
B-factors		
Protein	18.10	19.50
Ligand/ion	44.17	0
Water	26.30	34.10
R_{work}	0.16 (0.19)	0.15 (0.17)
R_{free}	0.19 (0.25)	0.20 (0.24)
No. of atoms		
Protein	1255	1179
Ligand/ion	6	0
Water	137	160
Root mean square bond lengths (Å)	0.007	0.006
Root mean square angle (°)	1.352	1.040
Ramachandran plot		
Favored (%)	98	98.67
Allowed (%)	2	1.33
Disallowed (%)	0	0

Next, we tested the secretion efficiency of the S3G-aleu-VSD-GFP. *Arabidopsis* protoplasts were transfected with wild-type, S3G, or I6G aleu-VSD-GFP. Protein gel blot analysis showed that all aleu-VSD-GFP was retained in the cells and none was not detected in the medium (Figure 3E). These results suggest that wild-type aleu-VSD-GFP was sorted correctly to the vacuoles by endogenous VSRs. In contrast, both S3G and I6G aleu-VSD-GFP resulted in secretion of the mutant proteins to the medium (18.4 and 37.5% secretion for S3G and I6G aleu-VSD-GFP, respectively) (Figure 3E). Taken together, our results strongly suggest that the S3G substitution, like the I6G substitution at the NPIR motif, affects cargo-receptor binding that lead to mis-sorting of aleu-VSD-GFP. Our results also imply that other domains of VSR1 are involved in recognizing the full-length of aleu-VSD, as Ile-6 of the aleurain peptide are disordered in the crystal structure and, presumably, make no interaction with the PA domain. This suggestion is consistent with a previous observation that both the PA and the Central domains of VSR are responsible for sequence-specific recognition of cargos (Cao et al., 2000).

The Invariant Arg-95 on the Cargo Binding Loop Is Crucial to Cargo Binding and Trafficking

As observed in the crystal structures, Ser-3 of the cargo-peptide forms a hydrogen bond with Arg-95. This invariant arginine residue is the only residue whose side chain takes part in cargo binding (Figure 1D). To test the role of Arg-95 in receptor-cargo interaction, we created a R95M mutant of VSR1NT and expressed it in *Arabidopsis* protoplasts (Figure 4). We showed that VSR1NT but not its R95M mutant was pulled down by Sepharose conjugated with the aleurain peptide (Figure 4B), suggesting that the R95M mutation abolished the interaction between VSR1NT and the aleurain peptide. Lysates from cells coexpressing aleu-VSD-GFP and VSR1NT or its R95M mutant were subjected to coimmunoprecipitation to further test the interaction of the R95M mutant with cargo protein. As shown in Figure 4C, R95M-VSR1NT was not detected in anti-T7 immunoprecipitates, indicating the interaction between the mutated protein and aleu-VSD-GFP was prevented. Taken together, these results suggest that the invariant residue Arg-95 on the cargo binding loop of the PA domain of VSR1 is crucial to cargo binding.

A previous study showed that the N-terminal lumenal region of VSR is involved in cargo binding that directs the cargo proteins to the vacuole (Humair et al., 2001). Replacing the N-terminal lumenal region with the GFP results in mis-sorting of cargo proteins, which become secreted into the medium (daSilva et al., 2005). Given that the R95M mutant failed to bind aleu-VSD-GFP, we thus questioned whether the R95M mutation in full-length VSR1 would lead to the secretion of cargo proteins. To test this hypothesis, CFP (cyan fluorescent protein)-tagged VSR1FL (CFP-VSR1FL) and its R95M mutant (R95M-CFP-VSR1FL) were generated (Figure 4A). In agreement with our hypothesis, the result showed that majority of aleu-VSD-GFP was sorted intracellularly in the presence of wild-type

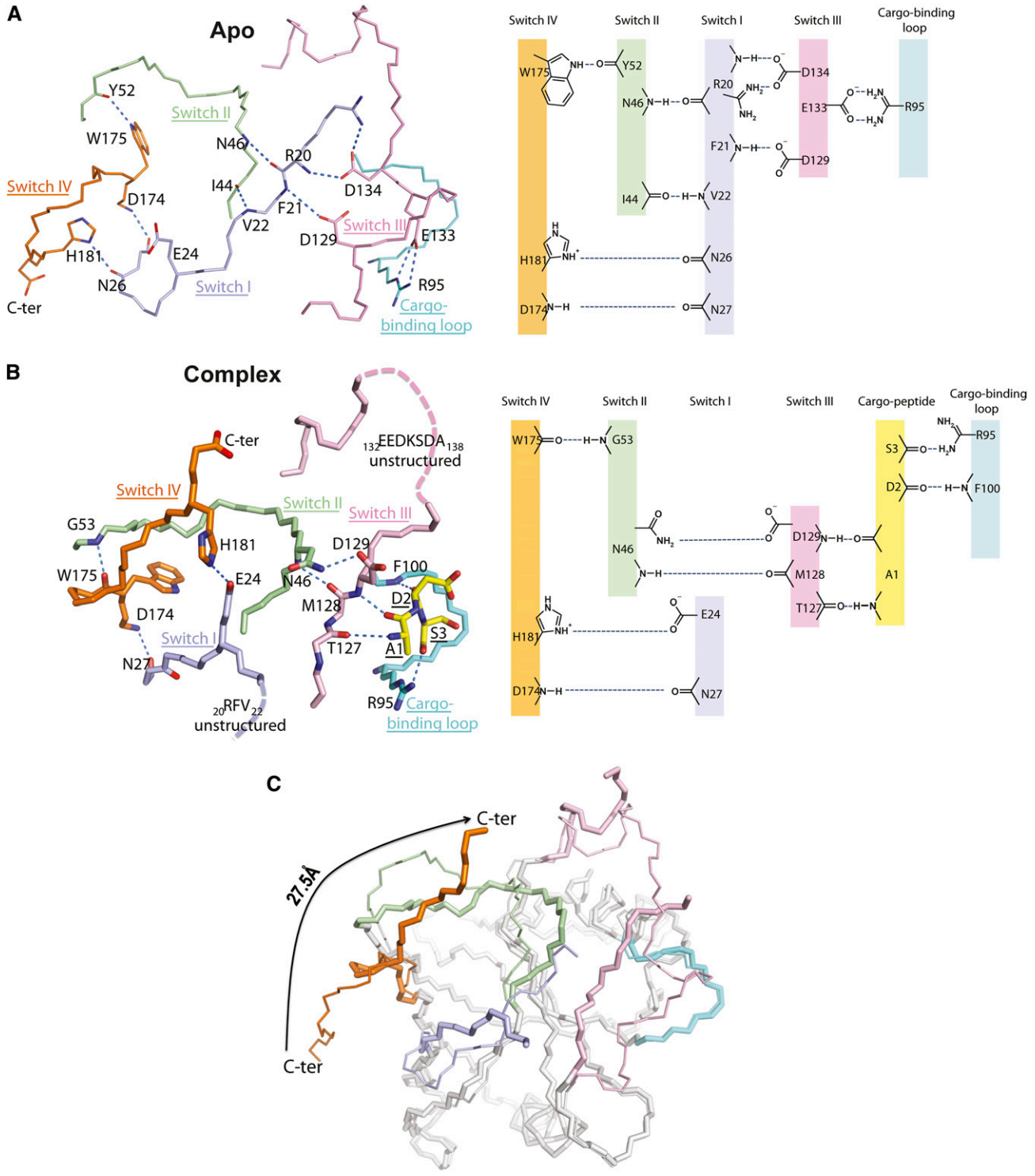

Figure 2. Cargo Binding Induces a Large Swivel Motion at the C Terminus of VSR1PA.

(A) and **(B)** The four switch regions are interconnected by a hydrogen bond network (dashed lines) in both apo **(A)** and complex **(B)** forms of VSR1PA. The binding of the aleurain cargo-peptide displaces the switch III residues from the cargo binding site and induces conformational changes that are propagated to the C terminus of VSR1PA via the hydrogen bond network. Upon cargo binding, residues R20-V22 and E132-A138 become unstructured and are indicated. The switch regions and the cargo binding loop are color-coded as indicated. A schematic representation of the hydrogen bond network is shown on the right.

(C) Superimposition of the structures of the apo (thin sticks) and complex (thick sticks) forms of VSR1PA, showing that binding of cargo induces a large swivel motion of ~27.5 Å that flips the C terminus by ~180°.

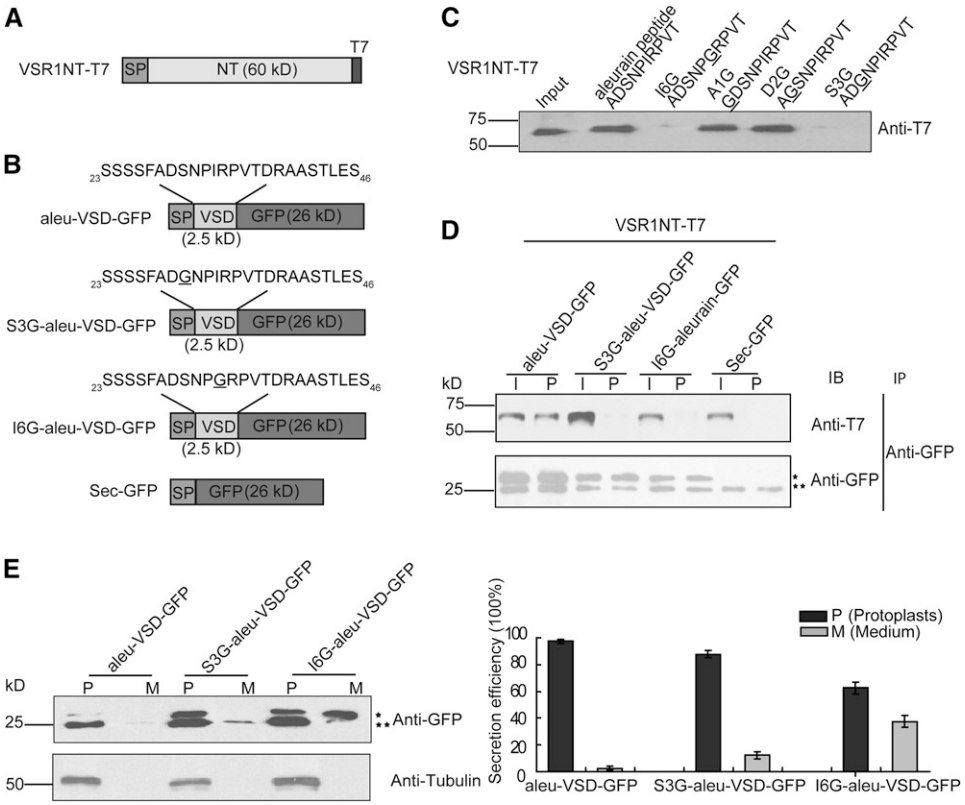

Figure 3. Residues Preceding the NPIR Motif Are Important in Cargo Binding and Trafficking.

(A) Construct of VSR1NT-T7, NT region of *Arabidopsis* VSR1 with its native signal peptide (SP), and a C-terminal T7 tag (Shen et al., 2013).
(B) Constructs used for aleu-VSD-GFP and its variants: aleu-VSD-GFP, previously described VSD from barley aleurain (Humair et al., 2001; Holwerda et al., 1992) following its native signal peptide; S3G-aleu-VSD-GFP and I6G-aleu-VSD-GFP, mutants of aleu-VSD-GFP, introduced mutation are underlined; Sec-GFP, the secreted form of GFP in which the signal peptide of sweet potato (*Ipomoea batatas*) sporamin was fused to GFP (Shen et al., 2013).
(C) Pull-down assay. *Arabidopsis* lysates expressing VSR1NT-T7 were mixed with sepharose conjugated with the aleurain cargo-peptide or its mutants. After extensive washing, the presence of bound VSR1NT-T7 was detected by protein gel blot analyses using anti-T7 antibodies. The sequences of the aleurain peptide and its mutants are shown on the top of the gel. Residue positions with glycine substitution are underlined.
(D) Coimmunoprecipitation assay. Protein extracts as input (I) were obtained from protoplasts cotransformed with the indicated constructs. Immunoprecipitation was performed using anti-GFP antibody. Immunoprecipitates (P) were analyzed by protein gel blot analysis with anti-T7 or anti-GFP antibody. Both the pull-down assay and coimmunoprecipitation assay indicated that S3G and I6G mutations abolished the receptor-cargo interaction in vitro.
(E) S3G and I6G mutations resulted in secretion of the aleu-VSD-GFP to the medium. Transiently expressed protoplasts with indicated constructs were collected 16 h after transformation. Protein extracts from protoplasts (P) and incubation medium (M) were analyzed by protein gel blot using anti-GFP or antitubulin antibodies. Absence of tubulin in the medium indicated that there was no protein leakage from protoplasts. In **(D)** and **(E)**, asterisk and double asterisks indicate the intact aleu-VSD-GFP and the processed GFP core, respectively. The histogram on the right reports the relative amount of proteins in the protoplasts and in the medium quantified using the ImageJ software. For quantification, we selected images that yielded a linear relationship between the intensity and exposure time. Three independent transformation experiments were performed. Error bars indicate SD (n = 3).

VSR1FL (Figures 4D and 4E). On the other hand, the R95M mutation resulted in a notable increase in secretion of aleu-VSD-GFP to the medium. Taken together, our results suggest that the R95M mutation prevents receptor-cargo interaction and leads to missorting of cargo proteins.

The Swivel Motion of the C-Terminal Tail of VSR1PA Is Crucial to Receptor-Cargo Recognition

In the crystal structure of apo-VSR1PA, the C-terminal tail points away from the cargo binding site. Binding of the cargo-peptide induces conformational changes in switch I-IV, causing the C-terminal tail of VSR1PA to undergo a swivel motion through ~180°, thus flipping toward the cargo binding site (Figure 2B). Since the C-terminal tail is connecting to the Central domain of VSR1, we hypothesize that such a swivel motion is crucial to receptor-cargo recognition by relocating the Central domain to the cargo binding site so that the Central domain can modulate the interaction with cargo proteins (Figure 5A). To test this hypothesis, we created a double mutant of VSR1NT (E24A/H181A). In the complex structure, the C-terminal tail is anchored to the PA domain by a hydrogen bond between two highly conserved residues, Glu-24 and His-181 (Figure 5A). We anticipated that the double mutations, E24A/H181A, will break the hydrogen bond, destabilize the bound

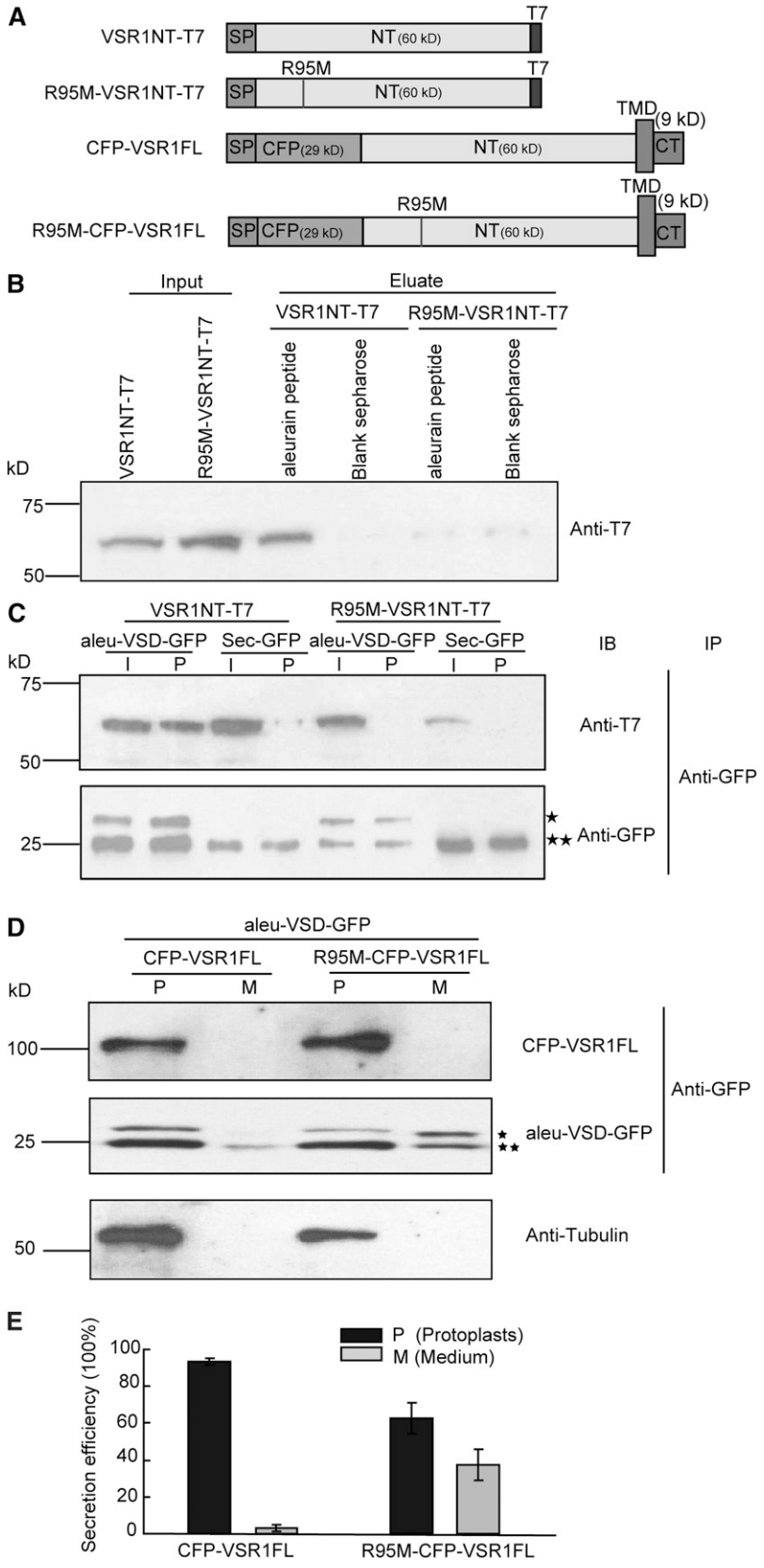

Figure 4. Arg-95 in the PA Domain of VSR1 Is Crucial for Cargo Binding and Trafficking.

(A) Constructs used: VSR1NT-T7, refer to Figure 3A; CFP-VSR1FL, CFP was inserted between the signal peptide (SP) and the full-length of *Arabidopsis* VSR1. The lumenal (NT), transmembrane (TMD), and C-terminal (CT) domains of VSR1 and the location of the R95M mutation are indicated.

conformation of the C-terminal tail and affect the binding of cargo protein. First, we tested the receptor-cargo interaction by coimmunoprecipitation. As shown in Figure 5B, no immunoprecipitates were detected from the E24A/H181A mutant, indicating that the hydrogen bond between the two residues is important for cargo binding. Next, we explored whether the double mutations would result in mis-sorting of aleu-VSD-GFP. Our results show that E24A/H181A resulted in an increase in secretion of aleu-VSD-GFP (18.5%) compared with the wild-type value of 7.4% (Figures 5C and 5D). Taken together, our results support the conclusion that the swivel motion of the C-terminal tail is crucial to cargo binding and trafficking.

Receptor-Cargo Recognition of Native Cargo and Barley Aleurain Followed the Same Rules

Using the VSD of barley (*Hordeum vulgare*) aleurain as a model cargo, we identified the following structural features that are crucial to receptor-cargo recognition and cargo trafficking: (1) residues preceding the NPIR motif of the VSD, (2) Arg-95 on the cargo binding loop of VSR1PA, and (3) the C-terminal tail conformation, stabilized by hydrogen bond between Glu-24 and His-181. Next, we questioned if these structural features are important in recognition of *Arabidopsis* native cargo. We recently identified a native cargo of At-VSR (CP), which is a putative cysteine protease harboring a NPIR motif at its N-terminal region (Shen et al., 2013). To test if the residues preceding the NPIR motif are important, we created a double mutant of CP (F32G/V33G), where the residues preceding the NPIR were mutated to glycine (Figure 6A). We showed that wild-type CP-GFP, but not the F32G/V33G mutant, was coimmunoprecipitated with VSR1NT. This observation suggests that residues preceding the NPIR motif of CP are important in receptor-cargo recognition (Figure 6B). Next, we tested if R95M and E24A/H181A mutants of VSR1NT can recognize the native cargo CP by coimmunoprecipitation (Figure 6C). Immunoprecipitates were detected with neither the R95M nor E24A/H181A mutant, indicating that these residues are also important for VSR1 binding with its native cargo, CP (Figure 6C). Taken together, our results showed that recognition of native cargo by At-VSR1 followed the same rules as that of the aleurain, suggesting the structure presented here can serve as a basis for understanding the interaction between VSRs and other cargo proteins.

DISCUSSION

The VSRs were identified based on their ability to bind soluble vacuolar proteins and transport them to the vacuole (Kirsch et al., 1994). The N-terminal region of VSR proteins, which consists of PA domain, Central domain, and EGF like repeats, is responsible for binding its cargo (Cao et al., 2000; Watanabe et al., 2002; Suen et al., 2010). Previous results demonstrate that sequence-specific binding of cargos requires both the PA and the Central domains (Cao et al., 2000). However, the molecular basis of VSR-cargo recognition is unclear. To fill this gap of knowledge, we determined the crystal structures of VSR1PA in its apo form and in complex with aleurain cargo peptide. Structural studies were complemented by pull-down assay and coimmunoprecipitation using VSR1NT protein derived from *Arabidopsis* cell lysates and by monitoring the mis-sorting (i.e., secretion) of cargo in *Arabidopsis* protoplasts. Our structural and functional studies have provided three important insights into how VSR recognizes its cargo:

First, the PA Domain Contains a Highly Conserved Cargo Binding Loop for Cargo Recognition

Residues $_{95}$RGDCYF$_{100}$ form a cradle that accommodates the incoming cargo-peptide (Figure 1D). In particular, Arg-95, which forms a hydrogen bond to Ser-3 of the cargo-peptide, plays a crucial role in cargo-receptor interaction, as the R95M mutation abolished cargo binding and resulted in protein mis-sorting in vivo (Figure 4). The PA domain of VSR is homologous to the lumenal region of another sorting receptor, receptor-homology-region-transmembrane-domain-RING-H2 proteins (RMR). In contrast to VSR, RMR does not contain the Central domain and the EGF repeats and only harbors a PA domain in its lumenal region (Park et al., 2005, 2007; Shen et al., 2011; Wang et al., 2011). It is interesting to point out that the sequence of the cargo binding loop is conserved among VSRs and RMRs, with a consensus sequence of RGxCxF (Supplemental Figure 4). Given the high similarity between VSR and RMR in this region, it is very likely that the RGxCxF motif would play similar role in receptor-cargo interaction in RMR.

Second, the PA Domain of VSR Recognizes the Sequences Preceding the NPIR Motif of VSD

It has been recognized long ago that the NPIR motif alone is not sufficient for vacuolar targeting. On the other hand, sequences

Figure 4. (continued).

(B) Pull-down assay. *Arabidopsis* lysates expressing VSR1NT-T7 or its mutant R95M-VSR1NT-T7 were mixed with sepharose with or without aleurain peptide conjugation. Eluate was analyzed by protein gel blot using anti-T7 antibodies. Aleurain peptide, sepharose conjugated with the aleurain peptide (ADSNPIRPVT); blank sepharose, sepharose without peptide conjugation.

(C) Coimmunoprecipitation assay. *Arabidopsis* protoplasts were cotransfected with constructs indicated, immunoprecipitated by anti-GFP antibodies, and analyzed by protein gel blot with T7 and GFP antibodies. Asterisk and double asterisks indicate the intact aleu-VSD-GFP and the processed GFP core, respectively. The R95M mutation abolished the receptor-cargo interaction in both pull-down assay and coimmunoprecipitation assay.

(D) Secretion of aleu-VSD-GFP. Protoplasts were transformed with aleu-VSD-GFP and CFP-VSR1FL or its R95M mutant. Protein extracts were prepared from transformed protoplasts (P) and incubation medium (M) and analyzed by protein gel blotting using GFP and tubulin antibodies. Absence of tubulin in the medium indicated that there was no protein leakage from protoplasts. Asterisk and double asterisks indicate the intact aleu-VSD-GFP and the processed GFP core, respectively.

(E) Histogram showing the relative amount of proteins in the protoplasts and in the medium quantified using the ImageJ software. To quantify the relative amount of proteins, three independent transformation experiments were performed and the error bars indicate SD (n = 3).

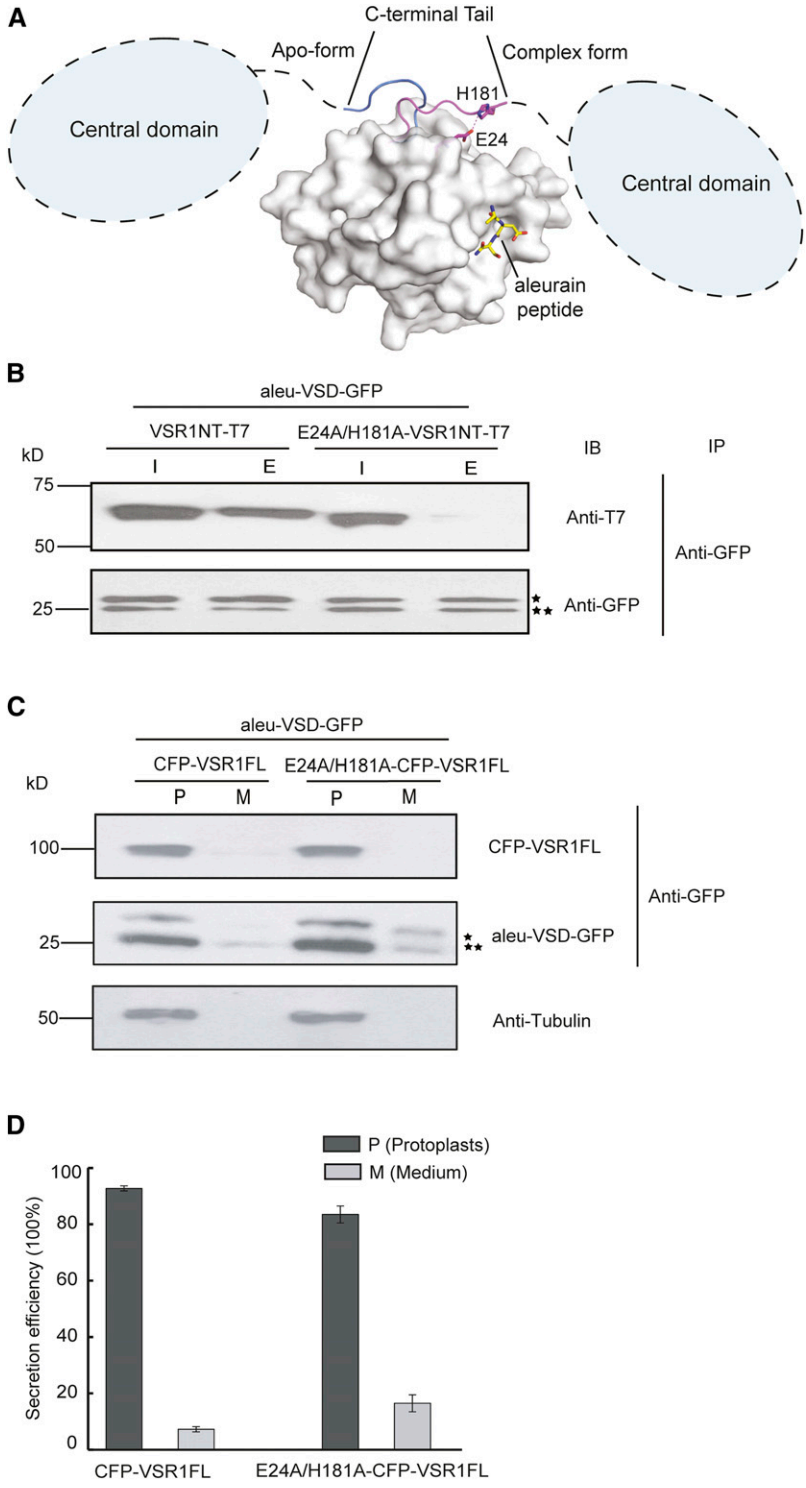

Figure 5. Conformational Changes at the C Terminus of VSR1PA Are Crucial for Receptor-Cargo Recognition.

(A) Binding of cargo-peptide induces the C-terminal tail of VSR1PA to flip ~180°. The bound conformation of the C-terminal tail is stabilized by a hydrogen bond between two conserved residues, Glu-24 and His-181. Such a swivel motion of the C terminus is expected to relocate the Central domain of VSR1 toward the cargo binding site.

on both flanks of the NPIR motif are important for vacuolar targeting (Holwerda et al., 1992). In this study, the complex structure reveals that VSR1PA interacts with the $_{1}$Ala-Asp-Ser$_{3}$ sequence preceding the NPIR motif of the aleurain cargo-peptide (Figure 1D). Mutagenesis studies show that the cargo recognition by the VSR1PA is sequence specific, as glycine substitution at Ser-3 position abolished the receptor-cargo interaction and resulted in mis-sorting of cargo in vivo (Figure 3). Taken together, our results suggest that binding of the Ala-Asp-Ser sequence to the PA domain of VSR is crucial to receptor-cargo recognition.

Residues $_{4}$NPIRPVT$_{10}$ of the aleurain peptide are disordered in the crystal structure of VSR1PA, suggesting that these residues undergo little interaction with the PA domain. As shown in our modeling analysis, these cargo residues clearly extend outside the cargo binding pocket of the PA domain, implying that the binding of these residues requires the participation of other domains of VSR (Supplemental Figure 5). It has been shown that a protease-digested fragment of BP-80, which contains the PA and the Central domain of VSR, is responsible for recognition of the NPIR-specific motif of cargos (Cao et al., 2000). In this study, we showed that both S3G and I6G mutation on the aleurain VSD abolished receptor-cargo interaction, suggesting that both domains cooperate to facilitate binding of cargos. This conclusion is also consistent with previous mutagenesis studies of VSDs (Neuhaus and Rogers, 1998; Ahmed et al., 2000; Cao et al., 2000). Taken together, it is likely that the PA domain and the Central domain each recognize a sequence motif within the VSD: The PA domain is responsible for binding the Ala-Asp-Ser sequence (preceding the NPIR motif), while the NPIR motif is recognized with the help of the Central domain.

Third, Binding of Cargo to the PA Domain Induces Conformational Changes That Result in Flipping the C Terminus of the PA Domain toward the Cargo Binding Site

A structural comparison between the apo and the complex form of VSR1PA reveals that cargo binding induces a large flipping motion of the C-terminal tail of VSR1PA (Figure 2; Supplemental Movie 1 and Supplemental Figure 2C). Such conformational changes are propagated from the cargo binding loop to the C terminus via conserved residues in switch I-IV regions. After cargo binding, the C-terminal tail is anchored to the PA domain by a hydrogen bond between two conserved residues Glu-24 and His-181 (Figure 2). Alanine substitution of these two residues abolished cargo binding and resulted in mis-sorting of cargo proteins (Figure 5), suggesting that the large flipping motion of the C-terminal tail of VSR1PA, which will bring the Central domain toward the cargo binding site, is essential for proper recognition and cargo sorting.

A Model of Receptor-Cargo Recognition by VSR

As residues involved in cargo binding and the conformational switches are highly conserved, the structural features identified for At-VSR1 should provide a paradigm for receptor-cargo interaction for how VSR recognize their cargo proteins. Summarizing our findings and previous work, we propose the following model (Figure 7). The PA domain of VSR is responsible for recognizing the residues preceding the NPIR motif. The cargo binding loop of the PA domain forms a cargo binding pocket that, in the case of barley aleurain, binds the peptide sequence Ala-Asp-Ser. Before cargo binding, the pocket is occupied by switch III residues and is in a closed conformation, and the C-terminal tail of the PA domain is pointing away from the cargo binding site. When the cargo protein is bound to the PA domain, the Ala-Asp-Ser sequence displaces the switch III residues from the pocket. Conformational changes at the cargo binding site are propagated to the C terminus of the PA domain. The resulting 180° flip of the C-terminal tail relocates the Central domain toward the cargo binding pocket and allows the Central domain to cooperate with the PA domain in recognizing the full-length vacuolar sorting determinant.

Sequence Preference of Recognition by the PA Domain

In this study, we showed that the $_{1}$Ala-Asp-Ser$_{3}$ sequence preceding the NPIR motif is recognized by the PA domain. There are several known NPIR-containing cargo proteins of VSR, and we modeled how the PA domain may interact with these cargo proteins. We showed that various sequences preceding the NPIR motif are well accommodated in the cargo binding pocket of the PA domain (Figure 7B). While we anticipate the sequence specificity to be loose because the PA domain forms only backbone hydrogen bonds to the cargo, we can identify some preference in these sequence positions. First, glycine is not favored at Ser-3 position. Based on our structure, there are potential interactions between the side chains at residue positions 2 and 3. For example, the hydroxyl group of Ser-3 can form a weak hydrogen bond to the carboxylate group of Asp-2. Glycine substitution may break the interaction and weaken the cargo binding. Moreover, glycine substitution is also unfavorable to binding because of entropic penalty (Krieger et al., 2005;

Figure 5. (continued).

(B) E24A/H181A mutant of VSR1NT failed to interact with aleurain. *Arabidopsis* lysates coexpressing aleu-VSD-GFP and VSR1NT-T7 or its E24/H181A mutant were immunoprecipitated (IP) with GFP-antibodies followed by immunoblot (IB) analysis on eluted proteins using GFP- or T7-antibodies. E, immunoprecipitates; I, 10% of input proteins.

(C) Secretion of aleu-VSD-GFP. Protein extracts were prepared from transformed protoplasts (P) and incubation medium (M) and analyzed by protein gel blotting using GFP and tubulin antibodies. Absence of tubulin in the medium indicated that there was no protein leakage from protoplasts. In **(B)** and **(C)**, asterisk and double asterisks indicate the intact aleu-VSD-GFP and the processed GFP core, respectively.

(D) Histogram showing the relative amount of proteins in the protoplasts and in the medium quantified using the ImageJ software. Error bars are the SD from three independent transformation experiments.

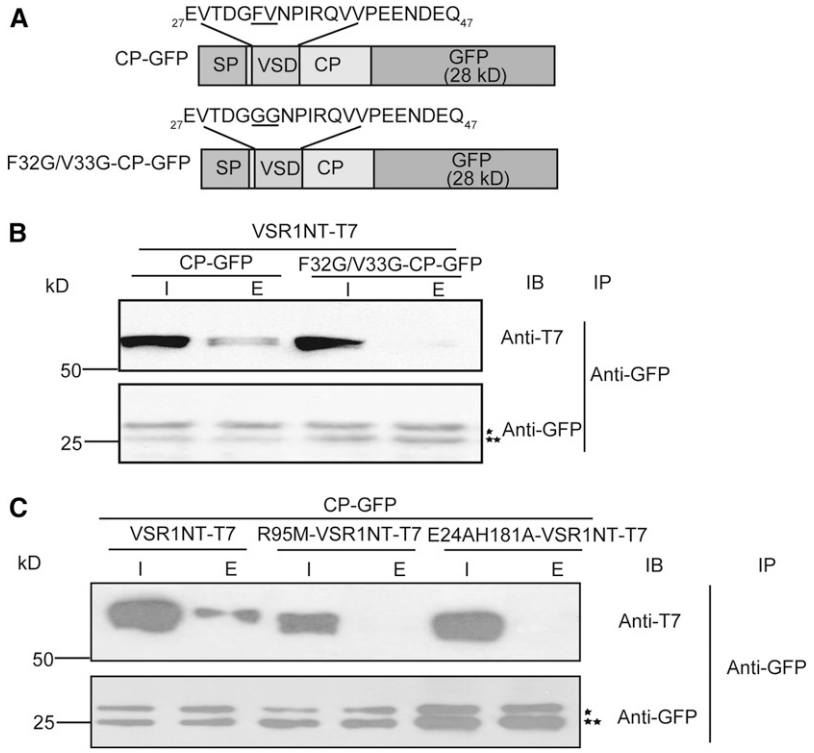

Figure 6. Recognition of Native Cargo by VSR1 Followed the Same Rules Derived from Barley Aleurain.

(A) Constructs used: CP-GFP, a native cargo of VSR, At4g16190 (CP) is fused with GFP.
(B) and **(C)** *Arabidopsis* protoplasts were cotransfected with VSR1NT-T7 and CP-GFP or their mutants as indicated. Lysates were immunoprecipitated (IP) with anti-GFP antibodies followed by immunoblot (IB) with anti-T7 and anti-GFP antibodies. In **(B)**, the mutated cargo protein, F32G/V33G-CP-GFP failed to interact with the VSR1NT-T7. In **(C)**, both the R95M and E24A/H181A mutants failed to interact with the cargo protein CP-GFP.

Scott et al., 2007). Second, proline is not allowed at the Ser-3 position. It is interesting to point out that the backbone ϕ dihedral angles of Ser-3 take values of $-158°$, which is not compatible with a proline residue, whose ring structure restricts the ϕ angle to $\sim -60°$. For a similar reason, proline is not favored at the Asp-2 position, which has a ϕ angle of $-93°$. In summary, because of the hydrogen bond that fixes the backbone conformation of the cargo-peptide, proline residues are not favored at either the Asp-2 or Ser-3 positions, implying that the proline residue in the NPIR motif cannot fit into the binding pocket of the PA domain. This observation is consistent with the suggestion that the PA and the Central domain each bind a separate motif within the VSD. As a result, the proline residue in the NPIR motif would be kept out of the binding pocket of the PA domain, ensuring cooperative binding of separate motifs within the VSD by both PA and Central domains.

In addition to the NPIR-containing VSD, which is often found in vacuolar lytic proteins, it has been reported that VSRs also bind to the C-terminal VSD (ctVSD) often found in proteins targeted to the protein storage vacuoles (Okita and Rogers, 1996; Kirsch et al., 1996; Watanabe et al., 2002; Suen et al., 2010; Shen et al., 2013). Unlike the NPIR-containing VSD, there is no obvious consensus sequence for ctVSD. However, it is common to find hydrophobic residues in ctVSD (Watanabe et al., 2002; Hunter et al., 2007; Suen et al., 2010). For example, the ctVSD of bean (*Phaseolus vulgaris*) phaseolin and Brazil nut (*Bertholletia excelsa*) 2S albumin contains the sequence of Ala-Phe-Val-Tyr and Ile-Ala-Gly-Phe, respectively (Saalbach et al., 1996; Hunter et al., 2007). It is interesting to point out that RMR, which contains only a PA domain in its lumenal region, also recognize the ctVSD (Park et al., 2005; Shen et al., 2011). It is likely that the PA domain of VSR is responsible for binding the ctVSD. Our modeling studies suggest that the ctVSDs of phaseolin and 2S albumin are well accommodated in the binding pocket of VSR1PA; the C-terminal carboxylate group of ctVSD may form a salt bridge with Arg-95, and the residues of the ctVSD may form hydrophobic interactions among themselves and with Tyr-99 on the cargo binding loop (Supplemental Figure 6).

Structural Insights into How pH May Affect Cargo Binding

It has been shown that acidic pH promotes dissociation of cargo from VSR in vitro (Kirsch et al., 1994; Ahmed et al., 2000; Watanabe et al., 2002). Cargo release by acidic pH is likely mediated by protonation of acidic residues. Within VSR1PA, we identified several candidate residues that may play a role in pH-dependent binding of cargo. For example, the invariant Arg-95 residue on the cargo binding loop is anchored into correct position for cargo binding by several salt bridges involving conserved acidic residues, Asp-94, Asp-119, and Glu-123 (Supplemental Figure 7). Protonation of these acidic residues by low pH may lead to

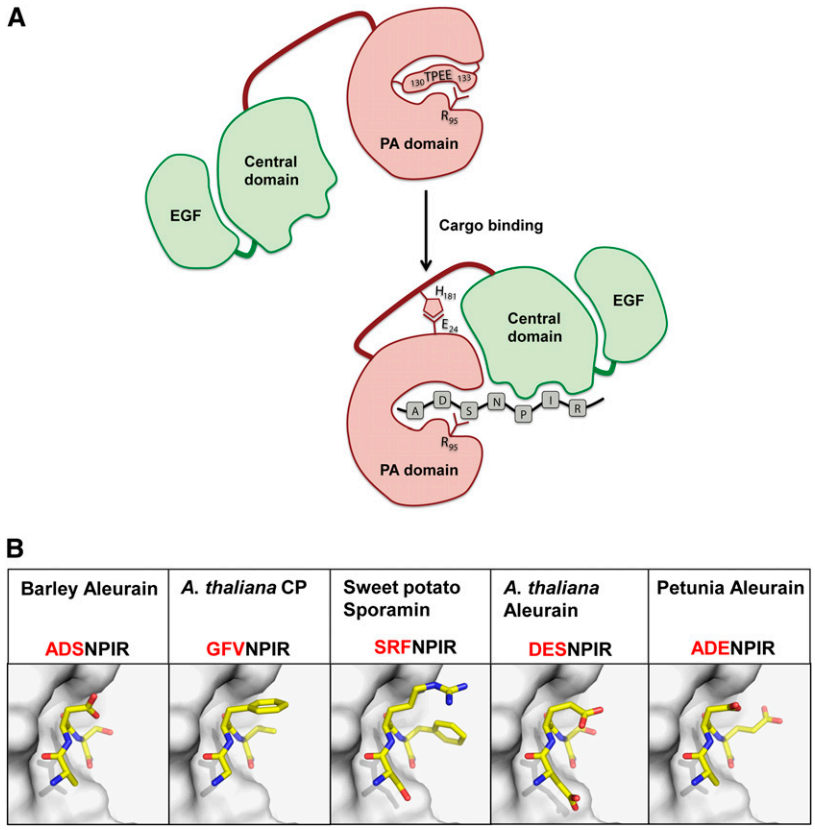

Figure 7. A Model for Cargo Recognition by VSRs.

(A) In the apo form, the cargo binding pocket of the PA domain is occupied by switch III residues ($_{130}$TPEE$_{133}$) and is in a closed conformation. The C-terminal tail of the PA domain points away from the cargo binding site so that the Central domain cannot cooperate with the PA domain on cargo binding. Residues (Ala-Asp-Ser in aleurain) preceding the NPIR motif are recognized by the PA domain. The invariant Arg-95 is crucial to receptor-cargo interaction by forming a hydrogen bond to the Ser residue. When these residues are bound to the PA domain, they displace the switch III residues from the cargo binding pocket and induce conformational changes that are propagated to the C terminus of the PA domain. The resulting 180° flip of the C-terminal tail, stabilized by hydrogen bond between Glu-24 and His-181, relocates the Central domain toward the cargo binding pocket and allows the Central domain to cooperate with the PA domain in recognizing the full-length VSD.

(B) Various sequences preceding the NPIR motif are well accommodated in the cargo binding pocket of the PA domain. Based on the crystal structure of VSR1PA in complex with the barley aleurain peptide ($_{1}$Ala-Asp-Ser$_{3}$), we have modeled the structure of VSR1PA in complex with various sequence motifs of *Arabidopsis* cysteine protease (Gly-Phe-Val) (Shen et al., 2013), sporamin (Ser-Arg-Phe) (Matsuoka and Nakamura, 1999), *Arabidopsis* aleurain (Asp-Glu-Ser) (Ahmed et al., 2000), and petunia (*Petunia hybrida*) aleurain (Ala-Asp-Glu) (Humair et al., 2001). The side-chain conformations of the residues without steric clashes were chosen from a backbone-dependent rotamer library.

a conformational change in Arg-95 and result in cargo release. Another possibility is the protonation of Glu-24, which may weaken the hydrogen bond between Glu-24 and His-18 and prevent the flipping motion that relocates the Central domain toward the cargo binding site.

In this study, we determined the crystal structure of VSR1PA and its complex with cognate cargo-peptide. Our work provide insights into a structural mechanism of how the PA domain and the Central domain cooperate to achieve sequence-specific binding of VSD, the sequence preceding the NPIR motif is important in inducing conformational changes in the PA domain that relocates the Central domain toward the cargo binding site. That either S3G or I6G mutation abolished receptor-cargo interaction suggests that the cooperation between the PA domain and the Central domain is important in sensing the full-length VSD. While our results demonstrated that the sequence preceding the NPIR motif is recognized by the PA domain, it remains elusive how the NPIR motif is recognized. There could be two possibilities. First, the Central domain contains a separate binding site for the NPIR motif. The relocation of the Central domain juxtaposes the two binding sites of the PA domain and the Central domain to achieve optimal binding of the VSD. Alternatively, the relocation of the Central domain may form a new binding cleft between the PA and Central domains for accommodating the NPIR motif. Structure determination of the full-length lumenal regions of VSR will further address the atomic detail of how the PA and the Central domains interact with the cargo proteins.

METHODS

Cloning, Expression, and Purification of VSR1PA

A DNA fragment of VSR1PA was amplified by PCR based on the *Arabidopsis thaliana* VSR1 sequence. Primers used to generate this construct are listed in Supplemental Table 1. VSR1PA was subcloned into an in-house pHisMBP vector, which contains the coding sequence of a six-Histidine-maltose binding protein (His6-MBP) tag, a 3C-like protease (SARS protease) cleavage site using *Bam*HI and *Sal*I restriction sites. Expression construct of VSR1PA encodes the 163-residue fragment corresponding to 20 through 182 of VSR1 with His6-MBP on its N terminus. The obtained clones were transformed into *Escherichia coli* SoluBL21 cells (Genlantis) for subsequent expression. Expression of recombinantVSR1PA was induced by 0.4 mM of isopropyl β-D-1-thiogalactopyranoside in *E. coli* strain SoluBL21 (Genlantis) during mid-log phase. The cells were induced at 25°C for 16 h, followed by sonication in buffer A (20 mM Tris, pH 8.0, 500 mM NaCl, and 1 mM TCEP). Soluble fraction was loaded onto a 5 mL HisTrap column (GE Healthcare), and the recombinant protein was eluted by buffer A with 300 mM imidazole. Protein was dialyzed against dialysis buffer (20 mM Tris, pH 7.4, 50 mM NaCl, 2 mM $CaCl_2$, and 1 mM TCEP) overnight at 4°C in the presence of SARS protease. The cleavage product mixture was further purified over a HisTrap column, and the flow-through fraction was collected. Finally, VSR1PA protein was purified to homogeneity using HiLoad 26/60 Superdex 75 column (GE Healthcare) in dialysis buffer.

Crystallization and Structure Determination

Apo VSR1PA was prepared in dialysis buffer and concentrated to 15 mg/mL. Crystals of VSR1PA were grown in 10% glycerol, 0.1 M MES, pH 6.0, 30% polyethylene glycol (PEG) 600, and 5% PEG 1000 at 16°C using the hanging-drop vapor diffusion method (Mikol et al., 1990). Iodide-derivative crystals of VSR1PA were obtained by quick soaking of native crystals in mother liquor containing an addition of 2 M potassium iodide. To obtain the structure of VSR1PA in complex with the aleurain peptide ($_1$ADSNPIRPVT$_{10}$), 15 mg/mL of VSR1PA protein in 20 mM Tris, pH 7.4, 50 mM NaCl, and 2 mM $CaCl_2$ were mixed with 5-fold molar excess of aleurain peptide and cocrystallized2 in 0.1 M HEPES, pH 7.0, and 25% PEG 6000 using the hanging drop vapor diffusion method. Crystals of VSR1PA complex were cryoprotected in mother liquor with an addition of 15% glycerol.

Diffraction data of both iodide derivative crystals and VSR1PA/aleurain cargo-peptide complex crystals were collected to 1.65 and 1.90 Å, respectively, using an in-house rotating anode x-ray generator (Rigaku FR-E+). Data for the iodide derivative crystal were integrated using XDS (Kabsch, 2010) driven by Xia2 (Winter, 2009). The structure was phased with SHELXC/D/E (Sheldrick, 2010) as implemented in HKL2MAP (Pape and Schneider, 2004) using the single-wavelength anomalous diffraction method. Six iodide sites were used to yield an interpretable electron density map. Data for the VSR1PA/aleurain complex were integrated with XDS and phased by the molecular replacement method using structure of apo VSR1PA as the search model. Molecular replacement was performed using PHASER driven by PHENIX.AUTOMR (Adams et al., 2010). Atomic structures of both apo and complex forms of VSR1PA were built using PHENIX.AUTOBUILD (Adams et al., 2010) followed by iterative rounds of interactive building using COOT (Emsley and Cowtan, 2004) and refinement using PHENIX.REFINE (Adams et al., 2010). The final models were validated with MOLPROBITY (Chen et al., 2010). Figures of protein structures were generated using PyMol (http://www.pymol.org).

Plasmid Construction for Functional Study in *Arabidopsis* Suspension Cells

Construction of the N-terminal lumenal region of *Arabidopsis* VSR1 (VSR1NT-T7) has been described previously (Suen et al., 2010; Shen et al., 2013). The N-terminal region of VSR1 sequence (VSR1NT) was obtained by PCR amplification with the T7 epitope tag added at its C terminus. The PCR-amplified VSR1NT fragment was digested with *Xba*I/*Sac*I and cloned into the plant expression vector pBI221 containing the cauliflower mosaic virus 35S promoter (Cui et al., 2014). All fluorescent fusion constructs used for transient expression in protoplasts were PCR amplified and cloned into the premade GFP/RFP/CFP backbone in pBI221. Mutations were introduced into various constructs using the QuikChange site-directed mutagenesis protocol (Stratagene). The primers used to generate various corresponding constructs are listed in Supplemental Table 1. The authenticity of all constructs was verified by DNA sequencing.

Protein Extraction from Transient Expressed Protoplasts

Transient expression using protoplasts derived from *Arabidopsis* suspension culture cells was performed according to previous reports (Miao and Jiang, 2007; Shen et al., 2013). Protein extraction was performed as described previously with some modifications (Zhuang et al., 2013). To prepare cell extracts from protoplasts, transformed protoplasts were first diluted 5-fold with 250 mM NaCl and then harvested by centrifugation at 300*g* for 5 min, followed by resuspension in the 1 mL binding buffer (25 mM HEPES, pH 7.1, 150 mM NaCl, 1 mM $MgCl_2$, and 1 mM $CaCl_2$) supplemented with 1× Complete Protease Inhibitor Cocktail (Roche). Protoplasts were sonicated five times for 1 s with 5-s intervals in an ice bath, followed by centrifugation at 14,000*g* for 30 min at 4°C. Supernatants were saved as input in the following experiments such as pull-down assay and coimmunoprecipitation assay.

Protein Preparation for the Secretion Assay

Transformed protoplasts together with the incubated medium were centrifuged at 300*g* for 5 min. The top layer containing the intact protoplasts was collected as intracellular fraction and subjected to the procedures of protein extraction from protoplasts as described in the last section. The remaining liquid fraction was saved to prepare the protein samples from the medium. One milliliter of medium was added to iCON concentrators (2 mL capacity, 3 kD MWCO; Pierce), prerinsed with the extraction buffer. Concentrators were centrifuged at 13,000*g* at 4°C until the volume of media was concentrated to 50 μL. Protein samples prepared from the protoplasts and the medium were subjected to SDS-PAGE followed by blotting to polyvinylidene fluoride membrane (Pall). The membranes were treated with antibodies against T7 (1:10,000; Abcam), GFP (Cui et al., 2014), or tubulin (1:4000; Roche). Immunoreactive signals were detected with an enhanced chemiluminescence detection system (ECL prime; Amersham Biosciences). The immunoblots were quantified by measuring the relative gray-scale intensity of the protein bands with ImageJ software (http://lukemiller.org/index.php/2010/11/analyzing-gels-and-western-blots-with-image-j/).

Pull-Down Assay

Synthetic peptides containing wild type VSD or their mutated forms were synthesized (GL Biochem). Construction of peptide-conjugated sepharose and pull-down assay were performed as described (Suen et al., 2010). Protein extracts prepared in the binding buffer were mixed with 10 μL peptide-conjugated sepharose at 4°C overnight. After extensive washing with binding buffer supplemented with 1% CHAPS, the sepharose containing the VSR1NT-peptide complex was boiled in 20 μL SDS-PAGE sample loading buffer for 5 min and subjected to protein gel blot.

Coimmunoprecipitation Assay

Coimmunoprecipitation assay was performed as described with some modifications (Zhuang et al., 2013). Protein extracts from protoplasts prepared in the binding buffer were incubated with GFP-TRAP magnetic

beads (ChromoTek) overnight at 4°C. Samples were extensively washed in binding buffer supplemented with 1% CHAPS and then eluted by boiling in SDS-PAGE sample loading buffer.

Accession Numbers

Sequence data from this article can be found in the Arabidopsis Genome Initiative or GenBank/EMBL databases under the following accession numbers: VSR1, Atg3g52850; CP, At4g16190. The atomic coordinates and structure factors have been deposited in the Protein Data Bank (PDB codes 4TJV and 4TJX, for apo form and aleurain peptide-bound structures, respectively).

Supplemental Data

The following materials are available in the online version of this article.

Supplemental Figure 1. Domain Organization of VSR.

Supplemental Figure 2. Most of the Conserved Residues of the PA Domain Are Localized on the Cargo Binding Loop and the Four Conformational Switch Regions.

Supplemental Figure 3. Electron Density Map of the Bound Aleurain Peptide.

Supplemental Figure 4. The Cargo Binding Loop of the PA Domain Is Conserved among VSRs and RMRs.

Supplemental Figure 5. Molecular Modeling Suggests That Residues in the NPIR Motif of the Cargo Protein Extend out of the Binding Pocket of VSR1PA.

Supplemental Figure 6. Modeling of interaction between ctVSD and VSR1PA.

Supplemental Figure 7. Salt Bridges That Anchor the Cargo Binding Residue, Arg-95, in Position.

Supplemental Table 1. Sequences of Oligonucleotides Used in This Study.

Supplemental Movie 1. Cargo Binding Induces a Large Flipping Motion at the C Terminus of VSR1PA

ACKNOWLEDGMENTS

We thank Kaming Lee and Kwok-Ho Chan and other members of the Jiang and Wong labs for helpful discussions. This study was supported by grants from the Research Grants Council of Hong Kong SAR (CUHK476212, CUHK2/CRF/11G, and AoE/M-05/12) and The Chinese University of Hong Kong Strategic Investment Scheme.

AUTHOR CONTRIBUTIONS

F.L. and K.-B.W. conceived and designed the experiments. F.L., Y.H.F., Y.Z., J.B.S., and K.-B.W. performed the experiments. F.L., L.J., and K.-B.W analyzed the data. F.L., L.J., and K.-B.W wrote the article.

Received July 13, 2014; revised August 14, 2014; accepted September 12, 2014; published September 30, 2014.

REFERENCES

Adams, P.D., et al. (2010). PHENIX: a comprehensive Python-based system for macromolecular structure solution. Acta Crystallogr. D Biol. Crystallogr. **66:** 213–221.

Ahmed, S.U., Rojo, E., Kovaleva, V., Venkataraman, S., Dombrowski, J.E., Matsuoka, K., and Raikhel, N.V. (2000). The plant vacuolar sorting receptor AtELP is involved in transport of NH (2)-terminal propeptide-containing vacuolar proteins in *Arabidopsis thaliana*. J. Cell Biol. **149:** 1335–1344.

Brown, C.K., Gu, Z.-Y., Matsuka, Y.V., Purushothaman, S.S., Winter, L.A., Cleary, P.P., Olmsted, S.B., Ohlendorf, D.H., and Earhart, C.A. (2005). Structure of the streptococcal cell wall C5a peptidase. Proc. Natl. Acad. Sci. USA **102:** 18391–18396.

Cao, X., Rogers, S.W., Butler, J., Beevers, L., and Rogers, J.C. (2000). Structural requirements for ligand binding by a probable plant vacuolar sorting receptor. Plant Cell **12:** 493–506.

Cereghino, J.L., Marcusson, E.G., and Emr, S.D. (1995). The cytoplasmic tail domain of the vacuolar protein sorting receptor Vps10p and a subset of VPS gene products regulate receptor stability, function, and localization. Mol. Biol. Cell **6:** 1089–1102.

Chen, V.B., Arendall III, W.B., Headd, J.J., Keedy, D.A., Immormino, R.M., Kapral, G.J., Murray, L.W., Richardson, J.S., and Richardson, D.C. (2010). MolProbity: all-atom structure validation for macromolecular crystallography. Acta Crystallogr. D Biol. Crystallogr. **66:** 12–21.

Cooper, A.A., and Stevens, T.H. (1996). Vps10p cycles between the late-Golgi and prevacuolar compartments in its function as the sorting receptor for multiple yeast vacuolar hydrolases. J. Cell Biol. **133:** 529–541.

Cui, Y., Zhao, Q., Gao, C., Ding, Y., Zeng, Y., Ueda, T., Nakano, A., and Jiang, L. (2014). Activation of the Rab7 GTPase by the MON1-CCZ1 complex is essential for PVC-to-vacuole trafficking and plant growth in Arabidopsis. Plant Cell **26:** 2080–2097.

daSilva, L.L.P., Foresti, O., and Denecke, J. (2006). Targeting of the plant vacuolar sorting receptor BP80 is dependent on multiple sorting signals in the cytosolic tail. Plant Cell **18:** 1477–1497.

daSilva, L.L.P., Taylor, J.P., Hadlington, J.L., Hanton, S.L., Snowden, C.J., Fox, S.J., Foresti, O., Brandizzi, F., and Denecke, J. (2005). Receptor salvage from the prevacuolar compartment is essential for efficient vacuolar protein targeting. Plant Cell **17:** 132–148.

De Marcos Lousa, C., Gershlick, D.C., and Denecke, J. (2012). Mechanisms and concepts paving the way towards a complete transport cycle of plant vacuolar sorting receptors. Plant Cell **24:** 1714–1732.

Emsley, P., and Cowtan, K. (2004). Coot: model-building tools for molecular graphics. Acta Crystallogr. D Biol. Crystallogr. **60:** 2126–2132.

Foresti, O., Gershlick, D.C., Bottanelli, F., Hummel, E., Hawes, C., and Denecke, J. (2010). A recycling-defective vacuolar sorting receptor reveals an intermediate compartment situated between prevacuoles and vacuoles in tobacco. Plant Cell **22:** 3992–4008.

Ghosh, P., Dahms, N.M., and Kornfeld, S. (2003). Mannose 6-phosphate receptors: new twists in the tale. Nat. Rev. Mol. Cell Biol. **4:** 202–212.

Holwerda, B.C., Padgett, H.S., and Rogers, J.C. (1992). Proaleurain vacuolar targeting is mediated by short contiguous peptide interactions. Plant Cell **4:** 307–318.

Humair, D., Hernández Felipe, D., Neuhaus, J.M., and Paris, N. (2001). Demonstration in yeast of the function of BP-80, a putative plant vacuolar sorting receptor. Plant Cell **13:** 781–792.

Hunter, P.R., Craddock, C.P., Di Benedetto, S., Roberts, L.M., and Frigerio, L. (2007). Fluorescent reporter proteins for the tonoplast and the vacuolar lumen identify a single vacuolar compartment in Arabidopsis cells. Plant Physiol. **145:** 1371–1382.

Jiang, L., and Rogers, J.C. (1998). Integral membrane protein sorting to vacuoles in plant cells: evidence for two pathways. J. Cell Biol. **143:** 1183–1199.

Jolliffe, N.A., Brown, J.C., Neumann, U., Vicré, M., Bachi, A., Hawes, C., Ceriotti, A., Roberts, L.M., and Frigerio, L. (2004).

Transport of ricin and 2S albumin precursors to the storage vacuoles of Ricinus communis endosperm involves the Golgi and VSR-like receptors. Plant J. **39:** 821–833.

Jørgensen, M.U., Emr, S.D., and Winther, J.R. (1999). Ligand recognition and domain structure of Vps10p, a vacuolar protein sorting receptor in Saccharomyces cerevisiae. Eur. J. Biochem. **260:** 461–469.

Kabsch, W. (2010). XDS. Acta Crystallogr. D Biol. Crystallogr. **66:** 125–132.

Kim, H., Kang, H., Jang, M., Chang, J.H., Miao, Y., Jiang, L., and Hwang, I. (2010). Homomeric interaction of AtVSR1 is essential for its function as a vacuolar sorting receptor. Plant Physiol. **154:** 134–148.

Kirsch, T., Paris, N., Butler, J.M., Beevers, L., and Rogers, J.C. (1994). Purification and initial characterization of a potential plant vacuolar targeting receptor. Proc. Natl. Acad. Sci. USA **91:** 3403–3407.

Kirsch, T., Saalbach, G., Raikhel, N.V., and Beevers, L. (1996). Interaction of a potential vacuolar targeting receptor with amino- and carboxyl-terminal targeting determinants. Plant Physiol. **111:** 469–474.

Krieger, F., Möglich, A., and Kiefhaber, T. (2005). Effect of proline and glycine residues on dynamics and barriers of loop formation in polypeptide chains. J. Am. Chem. Soc. **127:** 3346–3352.

Lam, S.K., Tse, Y.C., Jiang, L., Oliviusson, P., Heinzerling, O., and Robinson, D.G. (2006). Plant prevacuolar compartments and endocytosis. In Plant Cell Monographs, J. Šamaj, F. Baluška, and D. Menzel, eds (Berlin Heidelberg: Springer), pp. 37–61.

Matsuoka, K., Bassham, D.C., Raikhel, N.V., and Nakamura, K. (1995). Different sensitivity to wortmannin of two vacuolar sorting signals indicates the presence of distinct sorting machineries in tobacco cells. J. Cell Biol. **130:** 1307–1318.

Matsuoka, K., and Nakamura, K. (1999). Large alkyl side-chains of isoleucine and leucine in the NPIRL region constitute the core of the vacuolar sorting determinant of sporamin precursor. Plant Mol. Biol. **41:** 825–835.

Matsuoka, K., and Nakamura, K. (1991). Propeptide of a precursor to a plant vacuolar protein required for vacuolar targeting. Proc. Natl. Acad. Sci. USA **88:** 834–838.

Miao, Y., and Jiang, L. (2007). Transient expression of fluorescent fusion proteins in protoplasts of suspension cultured cells. Nat. Protoc. **2:** 2348–2353.

Miao, Y., Yan, P.K., Kim, H., Hwang, I., and Jiang, L. (2006). Localization of green fluorescent protein fusions with the seven Arabidopsis vacuolar sorting receptors to prevacuolar compartments in tobacco BY-2 cells. Plant Physiol. **142:** 945–962.

Mikol, V., Rodeau, J.L., and Giegé, R. (1990). Experimental determination of water equilibration rates in the hanging drop method of protein crystallization. Anal. Biochem. **186:** 332–339.

Motyka, B., Korbutt, G., Pinkoski, M.J., Heibein, J.A., Caputo, A., Hobman, M., Barry, M., Shostak, I., Sawchuk, T., Holmes, C.F., Gauldie, J., and Bleackley, R.C. (2000). Mannose 6-phosphate/insulin-like growth factor II receptor is a death receptor for granzyme B during cytotoxic T cell-induced apoptosis. Cell **103:** 491–500.

Nakamura, K., and Matsuoka, K. (1993). Protein targeting to the vacuole in plant cells. Plant Physiol. **101:** 1–5.

Neuhaus, J.M., and Rogers, J.C. (1998). Sorting of proteins to vacuoles in plant cells. Plant Mol. Biol. **38:** 127–144.

Okita, T.W., and Rogers, J.C. (1996). Compartmentation of proteins in the endomembrane system of plant cells. Annu. Rev. Plant Physiol. Plant Mol. Biol. **47:** 327–350.

Olson, L.J., Zhang, J., Dahms, N.M., and Kim, J.-J.P. (2002). Twists and turns of the cation-dependent mannose 6-phosphate receptor. Ligand-bound versus ligand-free receptor. J. Biol. Chem. **277:** 10156–10161.

Ottmann, C., Rose, R., Huttenlocher, F., Cedzich, A., Hauske, P., Kaiser, M., Huber, R., and Schaller, A. (2009). Structural basis for Ca^{2+}-independence and activation by homodimerization of tomato subtilase 3. Proc. Natl. Acad. Sci. USA **106:** 17223–17228.

Pape, T., and Schneider, T.R. (2004). HKL2MAP : a graphical user interface for macromolecular phasing with SHELX programs. J. Appl. Crystallogr. **37:** 843–844.

Paris, N., and Neuhaus, J.-M. (2002). BP-80 as a vacuolar sorting receptor. Plant Mol. Biol. **50:** 903–914.

Paris, N., Rogers, S.W., Jiang, L., Kirsch, T., Beevers, L., Phillips, T.E., and Rogers, J.C. (1997). Molecular cloning and further characterization of a probable plant vacuolar sorting receptor. Plant Physiol. **115:** 29–39.

Park, J., Oufattole, M., and Rogers, J. (2007). Golgi-mediated vacuolar sorting in plant cells: RMR proteins are sorting receptors for the protein aggregation/membrane internalization pathway. Plant Sci. **172:** 728–745.

Park, M., Lee, D., Lee, G.-J., and Hwang, I. (2005). AtRMR1 functions as a cargo receptor for protein trafficking to the protein storage vacuole. J. Cell Biol. **170:** 757–767.

Robinson, D.G. (2014). Trafficking of vacuolar sorting receptors: new data and new problems. Plant Physiol. **165:** 1417–1423.

Robinson, D.G., and Hinz, G. (1997). Vacuole biogenesis and protein transport to the plant vacuole : a comparison with the yeast vacuole and the mammalian lysosome. Protoplasma **197:** 1–25.

Rogers, S.W., Youn, B., Rogers, J.C., and Kang, C. (2004). Purification, crystallization and preliminary crystallographic studies of the ligand-binding domain of a plant vacuolar sorting receptor. Acta Crystallogr. D Biol. Crystallogr. **60:** 2028–2030.

Saalbach, G., Rosso, M., and Schumann, U. (1996). The vacuolar targeting signal of the 2S albumin from Brazil nut resides at the C terminus and involves the C-terminal propeptide as an essential element. Plant Physiol. **112:** 975–985.

Scott, K.A., Alonso, D.O., Sato, S., Fersht, A.R., and Daggett, V. (2007). Conformational entropy of alanine versus glycine in protein denatured states. Proc. Natl. Acad. Sci. USA **104:** 2661–2666.

Sheldrick, G.M. (2010). Experimental phasing with SHELXC/D/E: combining chain tracing with density modification. Acta Crystallogr. D Biol. Crystallogr. **66:** 479–485.

Shen, J., Suen, P.K., Wang, X., Lin, Y., Lo, S.W., Rojo, E., and Jiang, L. (2013). An in vivo expression system for the identification of cargo proteins of vacuolar sorting receptors in Arabidopsis culture cells. Plant J. **75:** 1003–1017.

Shen, Y., Wang, J., Ding, Y., Lo, S.W., Gouzerh, G., Neuhaus, J.-M., and Jiang, L. (2011). The rice RMR1 associates with a distinct prevacuolar compartment for the protein storage vacuole pathway. Mol. Plant **4:** 854–868.

Shimada, T., Fuji, K., Tamura, K., Kondo, M., Nishimura, M., and Hara-Nishimura, I. (2003). Vacuolar sorting receptor for seed storage proteins in *Arabidopsis thaliana*. Proc. Natl. Acad. Sci. USA **100:** 16095–16100.

Shimada, T., Kuroyanagi, M., Nishimura, M., and Hara-Nishimura, I. (1997). A pumpkin 72-kDa membrane protein of precursor-accumulating vesicles has characteristics of a vacuolar sorting receptor. Plant Cell Physiol. **38:** 1414–1420.

Suen, P.K., Shen, J., Sun, S.S.M., and Jiang, L. (2010). Expression and characterization of two functional vacuolar sorting receptor (VSR) proteins, BP-80 and AtVSR4 from culture media of transgenic tobacco BY-2 cells. Plant Sci. **179:** 68–76.

Tse, Y.C., Mo, B., Hillmer, S., Zhao, M., Lo, S.W., Robinson, D.G., and Jiang, L. (2004). Identification of multivesicular bodies as

prevacuolar compartments in *Nicotiana tabacum* BY-2 cells. Plant Cell **16:** 672–693.

Vitale, A and Raikhel, N. (1999). What do proteins need to reach different vacuoles? Trends Plant Sci. **4:** 149–155.

Vitale, A., and Hinz, G. (2005). Sorting of proteins to storage vacuoles: how many mechanisms? Trends Plant Sci. **10:** 316–323.

Wang, H., Rogers, J.C., and Jiang, L. (2011). Plant RMR proteins: unique vacuolar sorting receptors that couple ligand sorting with membrane internalization. FEBS J. **278:** 59–68.

Watanabe, E., Shimada, T., Kuroyanagi, M., Nishimura, M., and Hara-Nishimura, I. (2002). Calcium-mediated association of a putative vacuolar sorting receptor PV72 with a propeptide of 2S albumin. J. Biol. Chem. **277:** 8708–8715.

Watanabe, E., Shimada, T., Tamura, K., Matsushima, R., Koumoto, Y., Nishimura, M., and Hara-Nishimura, I. (2004). An ER-localized form of PV72, a seed-specific vacuolar sorting receptor, interferes the transport of an NPIR-containing proteinase in Arabidopsis leaves. Plant Cell Physiol. **45:** 9–17.

Winter, G. (2009). Xia2: an expert system for macromolecular crystallography data reduction. J. Appl. Crystallogr. **43:** 186–190.

Zhuang, X., Wang, H., Lam, S.K., Gao, C., Wang, X., Cai, Y., and Jiang, L. (2013). A BAR-domain protein SH3P2, which binds to phosphatidylinositol 3-phosphate and ATG8, regulates autophagosome formation in Arabidopsis. Plant Cell **25:** 4596–4615.